Electronic Supplementary Material (ESI) for Chemical Science.
This journal is © The Royal Society of Chemistry 2017

Electronic Supplementary Information

Near-Infrared Irradiation Triggered Target Strand Displacement Amplification for MicroRNA Analysis in Living Cells

Wenhao Dai,[ab] Haifeng Dong,*[ab] Keke Guo,[ab] and Xueji Zhang*[ab]

[a]*Beijing Key lab for Bioengineering & Sensing Technology, Research Center for Bioengineering & Sensing Technology, School of Chemistry and Bioengineering, University of Science & Technology Beijing, Beijing 100083, P.R.China*

[b] *National Institute of Precision Medicine & Health, Beijing, 100083, P. R. China*

Fax: (+) 86-10-82375840; E-mail: hfdong@ustb.edu.cn, zhangxueji@ustb.edu.cn

Experimental

Materials and reagents:

Hydrogen tetrachloroaurate (III) trihydrate ($HAuCl_4$) (99%), tris (carboxyethyl) phosphinehydrochloride (TCEP), and 3-(4,5-dimethyl-2-thiazolyl)-2,5-diphenyl-2-H- tetrazolium bromide (MTT) were purchased from Sigma-Aldrich (China). Hydrochloric acid (HCl), sodium borohydride ($NaBH_4$), Cetyltrimethylammonium bromide (CTAB, 99%), silver nitrate ($AgNO_3$), L-ascorbic acid ($C_6H_8O_6$), and dimethyl sulphoxide (DMSO) were obtained from Sinopharm Chemical Reagent Co., Ltd (Beijing, China) and methoxypoly (ethylene glycol) thiol (SH-PEG, 5 kDa) was purchased from Xiamen Sinopeg Biotech Co., LTD. Calcein-AM, PI and Hoechst 33342 were obtained from Invitrogen (USA). PBS (pH 7.4), fetal bovine serum (FBS), Dulbecco's modified Eagle's medium (DMEM), trypsin-EDTA and penicillin-streptomycin were purchased from Gibco Life Technologies (AG, Switzerland). All other chemicals used in this study were analytical reagent grade and used without further purification. Ultrapure water obtained from a Millipore water purification system (≥18 MΩ, Milli-Q, Millipore, Billerica, MA) was used in all runs.

The oligonucleotides were synthesized by Sangon Biological Engineering Technology & Co., Ltd (Shanghai, P. R. China) and purified using high-performance liquid chromatography. The DNA hairpins (MB and Assistant) were respectively annealed (heat at 95 °C for 5 min, gradually cool to 25 °C at 5 °C/min, and stand at 25 °C for 1 h at least) in PBS (10 mM, pH = 7.4, with 137 mM NaCl), ensuring the desirable secondary structures. The sequences were as follows:

Hairpin detection probe (HDP):

5' -ACA CCC CAA AAT CGA AGC ACT TCC CAT GTG TAG AGA AGT GCT TCG ATT T-3'

5'-SH $(CH_2)_6$ ACA CCC CAA AAT CGA AGC ACT TCC CAT GTG TAG AGA AGT GCT TCG ATT T-FAM-3'

Linker:

5'- GAA GTG CTC GGT GA-$(CH_2)_6$-SH -3'

Hairpin assistant probe [1]:

HAP-A 5’ -C ACT TCT CTA CAC ATG GGA AGT GCT TCG ATT TCC A TGT GTA GA -3’

HAP-B 5’ -AG C ACT TCT CTA CAC ATG GGA AGT GCT TCG ATT TCC A TGT GTA GA -3’

HAP-C 5’ -CG AG C ACT TCT CTA CAC ATG GGA AGT GCT TCG ATT TCC A TGT GTA GA -3’

HAP-D 5’ -AC CG AG C ACT TCT CTA CAC ATG GGA AGT GCT TCG ATT TCC A TGT GTA GA -3’

HAP-E 5’ -TC AC CG AG C ACT TCT CTA CAC ATG GGA AGT GCT TCG ATT TCC A TGT GTA GA -3’

HAP-D-FAM 5’ -AC CG AG C ACT TCT CTA CAC ATG GGA AGT GCT TCG ATT TCC A TGT GTA GAT-FAM-3’

All the RNA sequences were purchased from Shanghai Gene Pharma Co., Ltd. (Shanghai, PRC), purified using high-performance liquid chromatography and modified by 2'-hydroxy methylation. 2′-OMe modification can improve the nuclease resistance of single-stranded miRNA and keep it stable.[2] The sequence was listed as follows:

Target miRNA-373:

5’-GAA GUG CUU CGA UUU UGG GGU GU-3’

Instruments

The morphologies of AuNRs were examined with transmission electron microscopy (TEM) (using a JEM 2100 TEM microscope) at an acceleration voltage of 200 kV. The size distribution and zeta potential analysis were performed using a Zetasizer Nano ZS system (Malvern, UK), and the 633 nm laser was used for the dynamic Light Scattering (DLS). The UV-visible (UV-vis) absorption was acquired with a UV-1800 spectrophotometer (Shimadzu, Japan) and processed with Origin Lab software. All fluorescence measurements were performed on a Hitachi F-7000 fluorescence spectrofluorometer (Tokyo, Japan), while temperature was controlled by D77656 Hoffenberg Huber. A Veriti 96-Well Thermal Cycler-PCR machine (Applied Biosystems, USA) was used for temperature control involved in the enzyme reaction.

Synthesis of gold nanorods (AuNRs):

According to the typical seed-mediated, surfactant-assisted growth method in a two-step procedure, the AuNRs were synthesized as previously reported with brief modification.[3] Initially, seed solution was prepared by mixing aqueous solutions of CTAB (100 mM, 9.75 mL) and HAuCl4 (10 mM, 250 μL) at 30 ^{o}C. An aqueous solution of $NaBH_4$ (10 mM, 600 μL) was then added. This solution was aged 2 hours at room temperature. Next, a growth solution of CTAB (100 mM, 200 mL), $AgNO_3$ (10 mM, 2 mL), $HAuCl_4$ (100 mM, 1 mL), HCl (1 M, 700 μL)[4] and ascorbic acid (0.1 M, 1.1 mL) at 27 ^{o}C was prepared for subsequent use. Then, 240 μL of the seed solution was added to the growth solution under moderate stirring and left overnight at 27 ^{o}C. The nanorods were centrifugated at 13000 rpm for 15 min twice and washed with Ultrapure water. The AuNRs were characterized using TEM and UV–vis spectroscopy.

Stability measurements of THP-AuNRs assembly

In order to measure the colloidal stability under different solutions, water, high salt solution (phosphate buffered saline (PBS) 10 mM, pH = 7.4, with 137 mM NaCl) and cell medium were prepared and mixed with the THP-AuNRs assembly respectively. After incubation at room temperature for 2 weeks, the photoluminescence and absorption spectra of the samples were recorded.

Cell Culture:

MCF-7 and MDA-MB-231 cells were cultured in DMEM supplemented with 10% (v/v) FBS, 1% penicillin and streptomycin (100 U/mL) at 37 °C in a humidified atmosphere containing 5% CO_2. Cells that had been grown to subconfluence were dissociated from the surface with a solution of 0.25% trypsin/EDTA.

Multicellular tumor spheroids (MCTS) were cultured according to a reported method. Briefly, MCF-7 cells (10^5 /mL) with 20 μL were seeded on the inner surface of the lid for hanging a drop culture and 7 mL PBS was added into the bottom to the formate of a 100% humidity environment. Then, the MCF-7 cells were incubated for 3 days to grow into spheroids.

Cytotoxicity of multi-modified AuNRs:

MCF-7 cells and MDA-MB-231 cells (5.0×10^4) were cultured for 12 h in a 96-well plate

containing DMEM (100 μL) in each well, and then the medium was replaced with fresh serum-free medium (Opti-MEM) alone or medium containing different concentration of AuNRs-assistant-D/PEG/MB assembly and incubated for another 4 h. Next, MTT (20 μL, 5 mg/mL) was added to each well. The media were removed 4 h later, and DMSO (100 μL) was added to solubilize the formazan dye. After shocking (37 °C, 120 rpm) for 15 min, the absorbance of each well was measured using a Tecan Sunrise at 488 nm. The cytotoxicity of the laser was also investigated with the same procedure. The cytotoxicity of THP-AuNRs assembly was estimated by the percentage of growth inhibition calculated with the formula.

$$\text{Growth inhibition } \% = (1 - A_{text} / A_{control}) \times 100\%$$

Figures

One copy of target miRNA-373 could trigger unfolding of multiple HDP, resulting in amplified analysis fluorescence signals. When the target miRNAs are present in the cells, the stem of HDP will be unfolded. As a result, the concealed domain 3’ and 4 are exposed.

Then with HAP hybridization with HDP, target miRNAs is placed and released back to the next amplification circulation based on the toehold SDA mechanism.

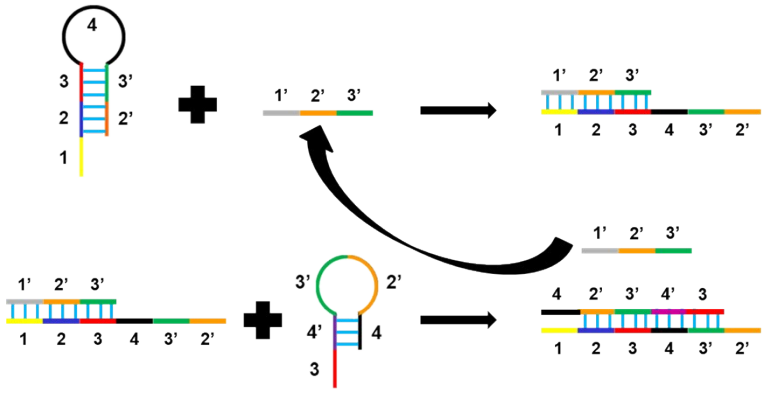

Figure S1. Principle of target miRNA-373 triggered nonenzymatic strand displacement amplification (SDA) reaction.

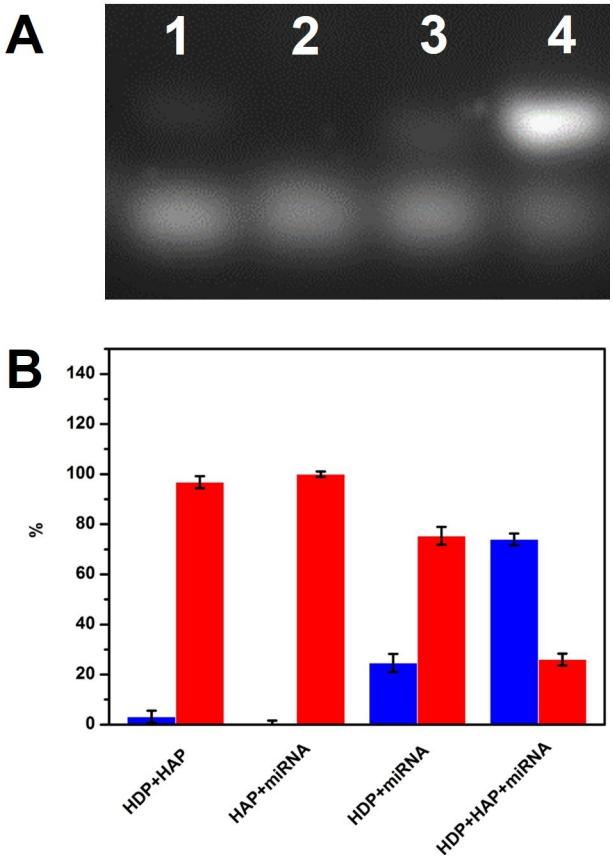

Figure S2. The hybridization efficiency of the verified experiment. A) The Gel electrophoresis results. Lane 1: HDP (1 μM) and HAP (1 μM); lane 2: HAP (1 μM) and miRNA-373 (1 μM); lane 3: HDP (1 μM) and miRNA-373 (1 μM); lane 4: HDP (1 μM), HAP (1 μM) and miRNA-373 (1 μM). B) The gray-scale ratio of different mixture, normalized with the negative control band intensity.

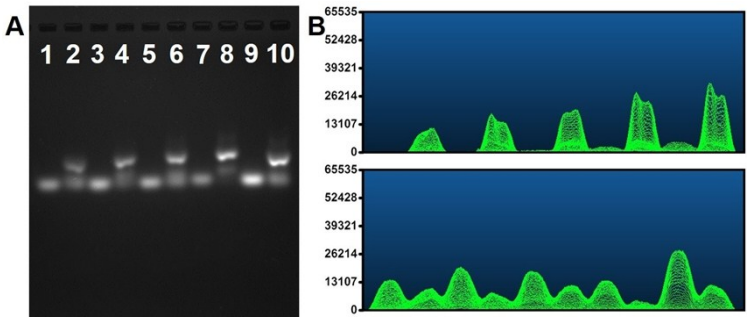

Figure S3. Gel electrophoresis optimized assistant experiments. A) The Gel electrophoresis results. Lane 1: HAP-A (1 μM); lane 2: HAP-A (1 μM) and linker (1 μM); lane 3: HAP-B (1 μM); lane 4: HAP-B (1 μM) and linker (1 μM); lane 5: HAP-C (1 μM); lane 6: HAP-C (1 μM) and linker (1 μM); lane 7: HAP-D (1 μM); lane 8: HAP-D (1 μM) and linker (1 μM); lane 9: HAP-E (1 μM); lane 10: HAP-E (1 μM) and linker (1 μM). B) The grey value analysis of the 10 lanes.

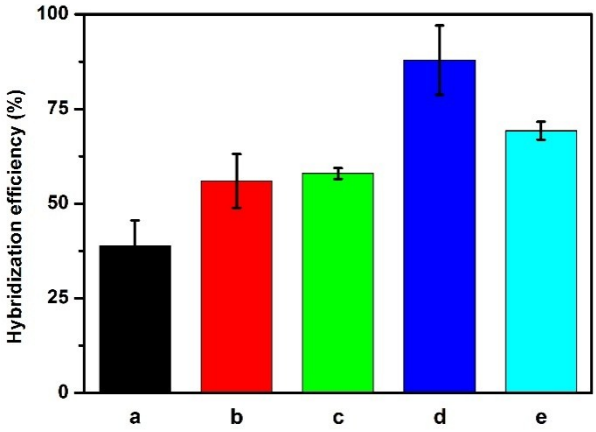

Figure S4. The hybridization efficiency of optimized assistant experiment, normalized with the negative control band intensity.

TEM characterization: The as-prepared AuNRs morphological information was characterized by transmission electron microscope (TEM) images. The generated AuNRs were monodispersed with average length and width of 49.71 ± 2.58 nm and 11.96 ± 0.98 nm, respectively (about 4.2:1 aspect ratio) using a modified seed-mediated method.[3,4]

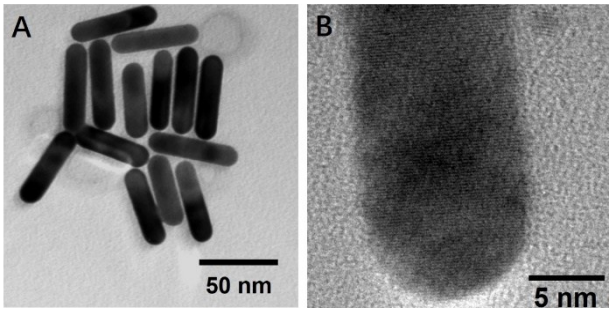

Figure S5. A) TEM image and B) HRTEM image of AuNRs.

UV-Vis characterization: The DNA was modified to the surface of AuNRs in three steps. Since the cetyltrimethylammonium bromide (CTAB) coating is thinner in their ends,[5,6] when the AuNRs are exposed to low concentrations of thiolated HAP-D first, the covalent attachment of the oligonucleotides occurs on the terminal surface of AuNRs. Then the SH-PEG (5000) was introduced to the side surface of AuNRs to stabilize and functionalize, and after that a high concentration of MB probe was added; allowing the sides CTAB of the AuNRs to be replaced sequentially. The as-prepared AuNRs had a strong longitudinal absorption peak at 816 nm and a transverse adsorption at 510 nm. After functionalizing with DNA, a 9 nm red shift associated with the change of a localized surface plasmon resonance effect and signal decrease were observed in a longitudinal absorption peak in the AuNRs nanoprobe, which indicated DNA was successfully modified on AuNRs.

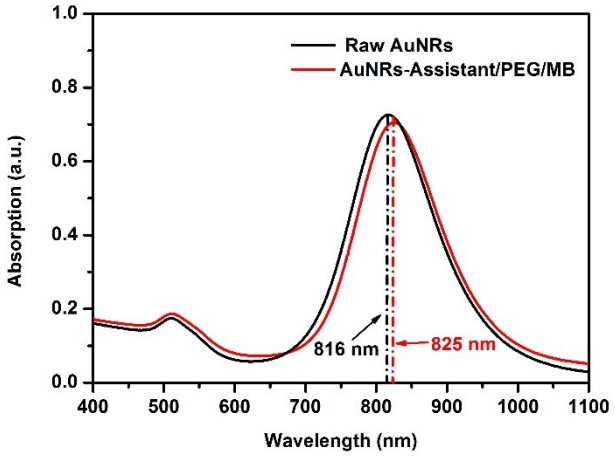

Figure S6. UV-vis spectra of AuNRs (50 μg/mL, black line) and AuNRs nanoprobe (50 μg/mL, red line).

DLS characterization: DLS was further employed to measure the hydrodynamic size of raw AuNRs and the AuNRs nanoprobe. It was found that the hydrodynamic size of 60 nm AuNRs increased to 75 nm after DNA conjugation in longitudinal orientation, suggesting the successful conjugation.

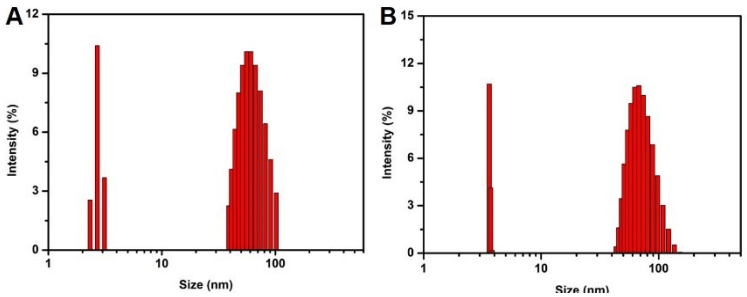

Figure S7. Hydrodynamic diameters distribution of A) AuNRs (50 μg/mL) and B) THP-AuNRs nanoprobe (50 μg/mL) in PBS (1×), respectively.

Zeta potentials characterization: It was observed that the negative-charged DNA and PEG conjugation procedure induced the zeta potential decrease, which further confirmed the successful assembly of the AuNRs nanoprobe.

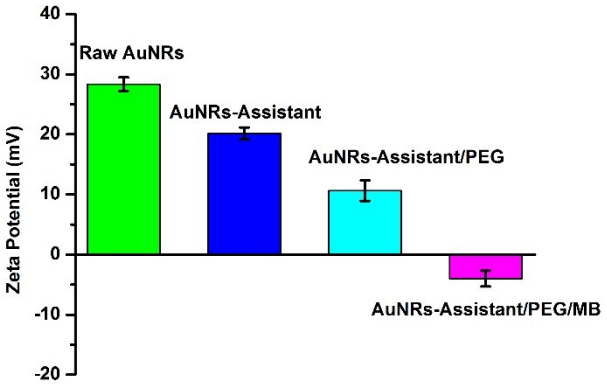

Figure S8. Zeta potentials of raw AuNRs (50 μg/mL), AuNRs-assistant (50 μg/mL), AuNRs-assistant/PEG (50 μg/mL) and AuNRs-assistant/PEG/MB (50 μg/mL).

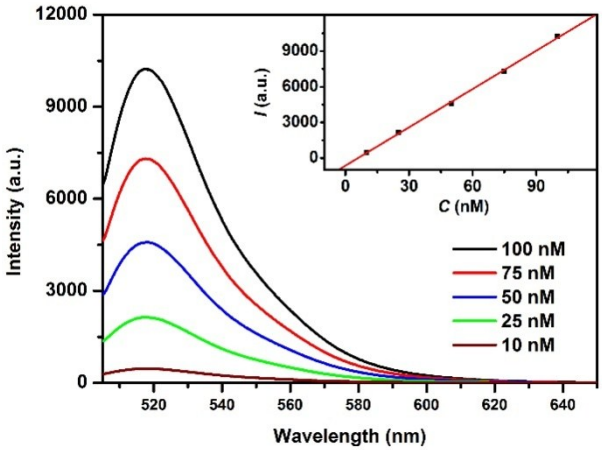

Figure S9. Determination of the average number of MB and assistant on each AuNRs using a DTT displacement assay. Inset is the standard curve of fluorescence intensity with different concentrations of TDP/TAP DNA sequences (FAM-label).

Stability of the THP-AuNRs nanoprobe: The obtained AuNRs nanoprobe exhibited excellent stability in aqueous solution, high salt solution (phosphate buffered saline (PBS) 10 mM, pH = 7.4, 137 mM NaCl), and cell medium for two weeks (Figure S10), while the UV−vis absorption (Figure S11) and PL spectra (Figure S12) of the THP-AuNRs nanoprobe have a little diminution after two weeks.

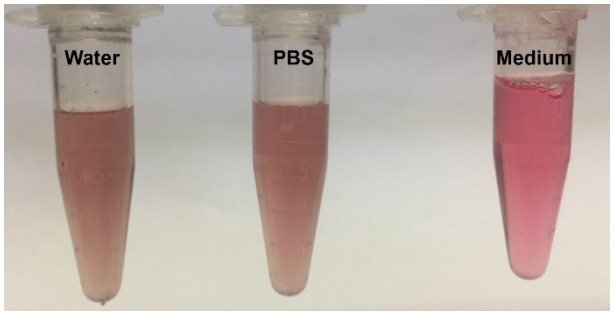

Figure S10. Photograph of the AuNRs nanoprobe in different media taken under visible light.

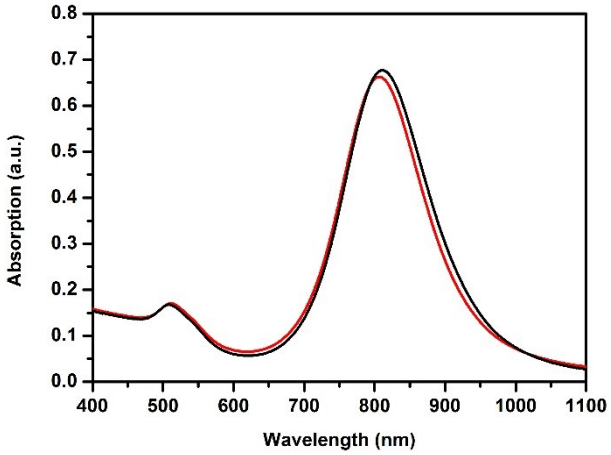

Figure S11. UV-vis spectra of AuNRs nanoprobe (50 μg/mL, black line) and after two weeks of THP-AuNRs nanoprobe (50 μg/mL, red line).

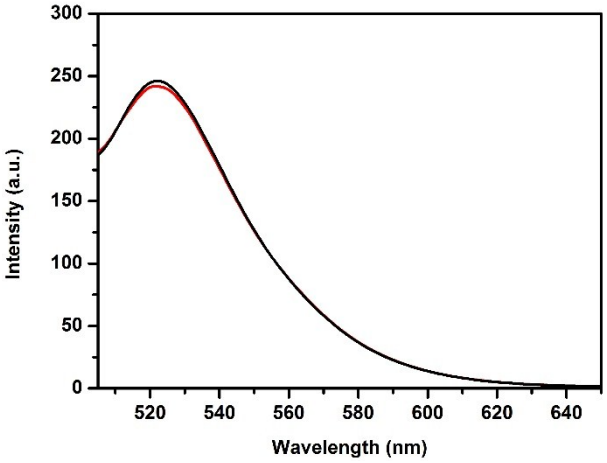

Figure S12. Fluorescence spectra of AuNRs nanoprobe (50 μg/mL, black line) and after two weeks of AuNRs nanoprobe (50 μg/mL, red line).

Photothermal conversion efficiency: In order to further investigate the photothermal transduction ability of the AuNRs nanoprobe aqueous solution; we recorded the temperature change of the sample (50 μg/mL) as a function of time under the 808 nm laser (0.64 W/cm^2) for 600 s. According to the obtained data, the photothermal conversion efficiency of the AuNRs nanoprobe can reach 27.82 %.

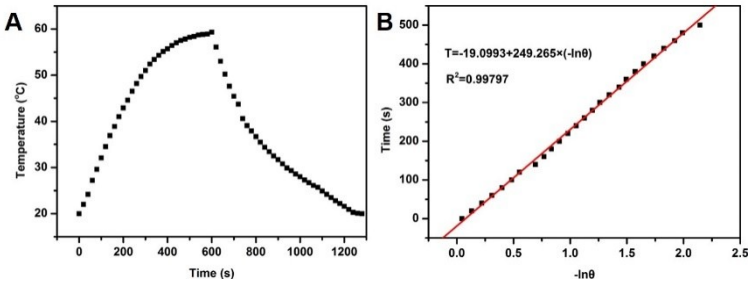

Figure S13. A) Photothermal effect of the AuNRs nanoprobe (50 μg/mL) when irradiated with an 808 nm laser (0.64 W/cm^2). The laser was turned off after irradiation for 10 min. B) Plot of cooling time versus negative natural logarithm of the temperature driving force obtained from the cooling stage as shown in (A).

Photothermal stability: Then, photothermal stability of the AuNRs nanoprobe was measured using a UV-Vis spectroscopic measurement by lengthening the irradiation time. A slight blue shift of the AuNRs nanoprobe SPR peak was observed during the first 20 min (Figure S14). When the irradiation time was more than 20 min, a large blue shift (51 and 70 nm, corresponding to 25 and 30 min, respectively) occurred in the longitudinal absorption peak of AuNRs, which suggested long time irradiation caused AuNRs longitudinal melting.[7,8] The TEM data and corresponding size statistics were also confirmed that our AuNRs nanoprobe was photothermally stable during the whole experiment process exposed to 3 min irradiation for miRNA detection (Figure S15 and S16).

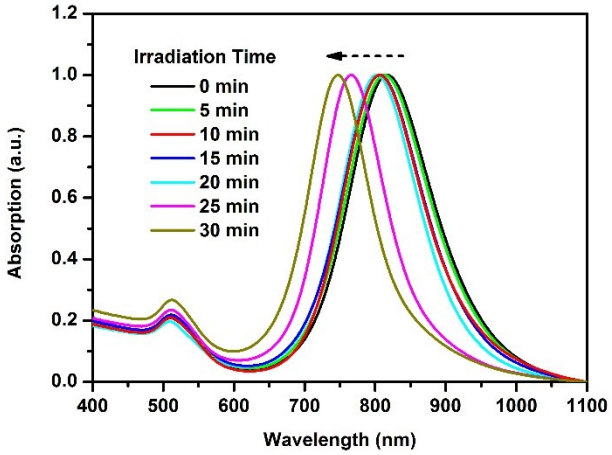

Figure S14. The Uv-vis absorbance spectrum of AuNRs nanoprobe (50 μg/mL) under the 808 nm laser irradiation.

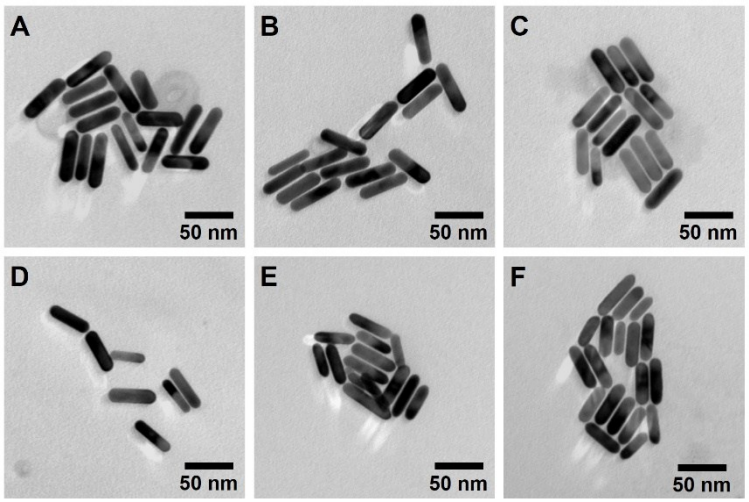

Figure S15. The TEM images of AuNRs nanoprobe with different irradiation time. A) 5 min, B) 10 min, C) 15 min, D) 20 min, E) 25 min, F) 30 min.

Reaction time	Length	Diameter	Aspect ratio
0 min	49.71±2.58	11.96±0.98	4.18±0.36
5 min	49.63±4.60	12.15±1.26	4.11±0.40
10 min	49.73±3.33	12.07±1.10	4.15±0.43
15 min	49.35±3.29	12.12±1.18	4.07±0.34
20 min	49.41±3.87	12.62±1.09	3.93±0.29
25 min	48.03±4.39	13.10±1.07	3.69±0.34
30 min	46.48±2.56	13.18±0.96	3.54±0.23

Figure S16. The average length and width of a AuNRs nanoprobe with different irradiated time.

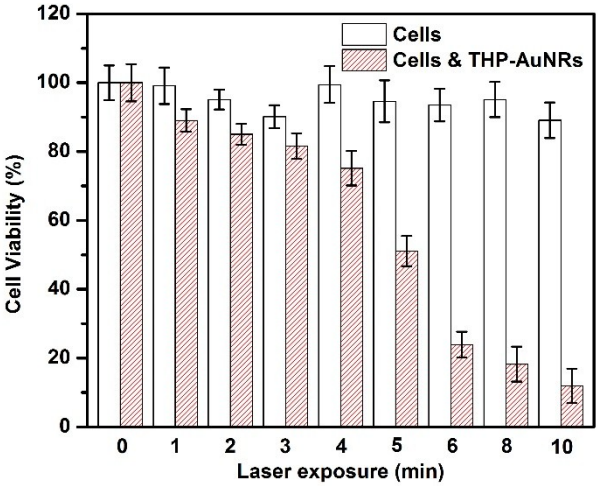

Figure S17. Cell viabilities of MDA-MB-231 cells after the AuNRs nanoprobe induced PTT for different lengths of time.

Quantify intracellular miRNA-373: In order to quantify the quantity of intracellular miRNA-373 in single MCF-7, MDA-MB-231 and NHDF cells, a different quantity of miRNA-373 mimics were transfected into a single MCF-7 cell, and we detected the intracellular intensity to more than 100 cells, respectively (Table S1). Given the endogenous miRNA and mimics miRNA displayed equal hybridization with THP-AuNRs nanoprobe and all the mimics were completely transfected into the cells, the calibration plots showed a good linear relationship between the relative fluorescence intensity and the quantity of miRNA-373 mimics with a linear equation of F(au) = $0.6758m_{mimics}$ (R^2=0.99705). From the linear regression equation and fluorescence intensity (Table S2), we calculated the intracellular miRNA-373 concentration in each cell line.

	m_{mimics}	PL Intensity	Relative PL Intensity
1	0	1033	
2	825	1502	469±121
3	1650	2190	1157±78
4	3300	3337	2304±237
5	4950	4361	3328±89

Table S1. The quality of mimics and corresponding PL intensity in a single MCF-7 cell.

Cell Type	PL Intensity	m_{mimics}	m_{miRNA}
MCF-7	1033±156	1528±231	764±116
MDA-MB-231	2071±132	3064±196	1532±98
NHDF	120±34	178±51	89±26

Table S2. Calculations of the quality of miRNA-373 in single MCF-7, MDA-MB-231, and NHDF cells.

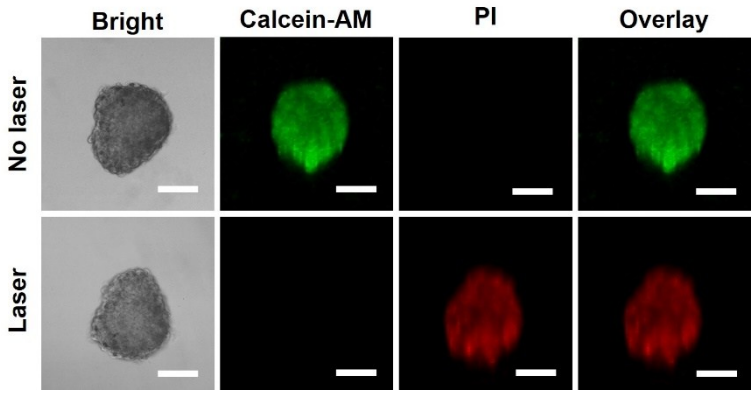

Figure S18. Three-dimensional confocal fluorescence reconstruction images. The MCTS were all costained by Calcein-AM (live: green) and PI (dead: red). Scale bars: 50 μm.

References

1 S. Yamano, J. Dai, S. Hanatani, K. Haku, T. Yamanaka, M. Ishioka, T. Takayama, C. Yuvienco, S. Khapli, A. M. Moursi and J. K. Montclare, *Biomaterials*, 2014, **35**, 1705-1715.

2 J. Krützfeldt, S. Kuwajima, R. Braich, K. G. Rajeev, J. Pena, T. Tuschl, M. Manoharan and M. Stoffel, *Nucleic Acids Res.*, 2007, **35**, 2885-2892.

3 N. J. Durr, T. Larson, D. K. Smith, B. A. Korgel, K. Sokolov and A. Ben-Yakar, *Nano Lett.*, 2007, **7**, 941-945.

4 Z. R. Guo, C. R. Gu, X. Fan, Z. P. Bian, H. F. Wu, D. Yang, N. Gu and J. N. Zhang, *Nanoscale Res. Lett.*, 2009, **4**, 1428-1433.

5 L. Wang, Y. Zhu, L. Xu, W. Chen, H. Kuang, L. Liu, A. Agarwal, C. Xu and N. A. Kotov, *Angew. Chem. Int. Ed.*, 2010, **49**, 5472-5475.

6 J. Wang, G. Z. Zhu, M. X. You, E. Q. Song, M. I. Shukoor, K. J. Zhang, M. B. Altman, Y. Chen, Z. Zhu, C. Z. Huang and W. H. Tan, *ACS Nano*, 2012, **6**, 5070-5077.

7 C.-C. Chen, Y.-P. Lin, C.-W. Wang, H.-C. Tzeng, C.-H. Wu, Y.-C. Chen, C.-P. Chen, L.-C. Chen and Y.-C. Wu, *J. Am. Chem. Soc.*, 2006, **128**, 3709-3715.

8 A. Wijaya, S. B. Schaffer, I. G. Pallares and K. Hamad-Schifferli, *ACS Nano*, 2009, **3**, 80-86.